Proceedings of the 9th U.S. National and 10th Canadian Conference on Earthquake Engineering
Compte Rendu de la 9ième Conférence Nationale Américaine et
10ième Conférence Canadienne de Génie Parasismique
July 25-29, 2010, Toronto, Ontario, Canada • Paper No 571

SYSTEM IDENTIFICATION BY INTRODUCING A NEW ENHANCED HILBERT-HUANG TRANSFORM METHOD

O. Bahar[1] and S. Ramezani[2]

ABSTRACT

Hilbert-Huang transform (HHT) is a powerful signal processing method, which consists of two main steps; the empirical mode decomposition (EMD) and Hilbert spectral analysis (HSA). There are two mathematical limitations that restrict applying the Hilbert transform. In this paper, a new enhanced Hilbert-Huang transform (EHHT) is proposed in which the limitations of the Hilbert spectral analysis are circumvented. Furthermore, based on the proposed EHHT a new output-only system identification method is proposed. By using the new method, ambient response data of an arch bridge (Beichuan Bridge) is analyzed and the first six frequencies and mode shapes are identified. Results demonstrate that in contrary to HHT, EHHT can be successfully applied in identification process. Proposed identification method by employing the EHHT is an effective tool for future researches in the field of system identification.

Introduction

System identification is an important subject in the field of civil engineering. Structural system identification methods specifically employ theoretical principals of both signal processing and structural dynamics in which the former plays more significant role. Up to now, many signal processing methods have been proposed to have a wide range of applicability and overcome the previous methods drawbacks. Hilbert-Huang transform (HHT) is one of the recently proposed methods which is developed by Huang et al. (1998) to deal with nonstationarity and nonlinearity in signals. Based on HHT, Yang et al. (2003) and (2004) have identified some main characteristic features of structures.

The HHT consists of two steps; the empirical mode decomposition (EMD) and the Hilbert spectral analysis (HSA). Considerable researches has been carried out to improve HHT performance, but in most of them focus is on the first step, *i.e.* EMD (Huang et al. 1999, Deering et al. 2005, Sharpley et al. 2006) and less work has been done on the second step, *i.e.* HSA (Huang and Bethesda 2005). To achieve physically meaningful instantaneous frequency through the Hilbert transform, the definition of an IMF is only a necessary condition and the requirements of the Bedrosian and Nuttall theorems is needed to be fulfilled (Huang and Bethesda, 2005). Huang and Bethesda (2005) proposed the normalized amplitude Hilbert transform (NAHT) method to consider requirements of the Bedrosian theorem. This method determines a normalized IMF

[1] Assist. Prof., Structural Eng. Dept., International Institute of Earthquake Engineering and Seismology (IIEES), Tehran, Iran
[2] MSc Graduate in Earthquake Engineering, Structural Eng. Dept., IIEES, Tehran, Iran

(Carrier wave), but the requirement of the Nuttall theorem has not been considered yet. Furthermore, Huang (2005) mentioned that using arc-cosine function, instead of the Hilbert transform, results in a more accurate phase function. In this case another difficulty arises. Due to the imperfect normalization process, carrier wave can take values out of [–1,1]. Therefore, arc-cosine cannot be applied to the imperfect carrier wave.

In this paper, first a five-step method developed by the authors, named the enhanced Hilbert-Huang transform (EHHT) is proposed in which the arc-cosine is used to get the phase function instead of the Hilbert transform (Bahar and Ramezani 2009, Ramezani 2009). Then, based on the proposed EHHT and through a case study an output-only system identification method is presented (Ramezani 2009). In this method, natural frequencies are estimated from an averaged marginal spectrum and then the corresponding mode shapes are extracted with a remarkable accuracy. To highlight the differences between the classic and the enhanced HHT methods, a brief description of the classic Hilbert-Huang transform and its limitations is presented in the following sections.

The classic Hilbert-Huang transform and its limitations

As it is mentioned, the HHT consists of two steps; the EMD and the HSA. First, EMD as a key part fulfills necessary conditions in order to utilize HSA. Then, HSA presents amplitude-frequency-time distribution of the signal through the Hilbert transform, designated as a Hilbert spectrum.

Empirical mode decomposition

EMD is an algorithm and does not admit an analytical definition. The EMD decomposes a signal to a finite number of oscillatory modes which called intrinsic mode functions (IMFs). By definition, an IMF is any function that satisfies two conditions: (1) in the whole data set, the number of extremes and the number of zero crossings must either equal or differ at most by one; and (2) at any point, the mean value of the envelope defined by the local maxima and the envelope defined by the local minima is zero.

For a given signal, $x(t)$, with at least one maximum and one minimum, the EMD procedure can be summarized in five steps as follows; (1) identify all the local extrema, (2) connect all the local maxima by a cubic spline interpolant as the upper envelope, $e_{\max}(t)$, and repeat the procedure for the local minima to achieve the lower envelope, $e_{\min}(t)$, (3) compute the average: $m_1(t) = [e_{\max}(t) + e_{\min}(t)]/2$, (4) let $h_1(t) = x(t) - m_1(t)$, if $h_1(t)$ is not an IMF, repeat steps 1 to 3 on $h_1(t)$ to obtain the first IMF, $c_1(t)$, (5) define $r_1(t) = x(t) - c_1(t)$; and repeat steps 1 to 5 on $r_1(t)$ to extract n IMFs. At the end, $x(t)$ is decomposed to n-separate IMFs and a residue, r_n, which is either a mean trend or a constant. Therefore, $x(t)$ can be defined as Eq. 1. Among the IMFs, c_1 has the highest frequency content and c_n has the lowest one.

$$x(t) = \sum_{i=1}^{n} c_i(t) + r_n(t) \tag{1}$$

Hilbert spectral analysis

For any real-valued function $c(t)$ of L^P class, the Hilbert transform, $y(t)$, is defined by:

$$y(t) = \frac{1}{\pi} P \int_{-\infty}^{\infty} \frac{c(\tau)}{t-\tau} d\tau \tag{2}$$

where P indicates the principal value of the singular integral. With the Hilbert transform, the analytic signal, $z(t)$, is defined as:

$$z(t) = c(t) + i\, y(t) = A(t)\, e^{i\theta(t)} \tag{3}$$

in which

$$A(t) = \sqrt{c^2(t) + y^2(t)} \qquad , \qquad \theta(t) = \arctan\left(\frac{y(t)}{c(t)}\right) \tag{4}$$

where $A(t)$ and $\theta(t)$ stand for instantaneous amplitude (envelope) and the phase function, respectively. Instantaneous frequency is defined as derivative of the phase function:

$$f(t) = \frac{1}{2\pi} \frac{d\theta(t)}{dt} \tag{5}$$

Having above definitions, $c(t)$, can be written as:

$$c(t) = \Re(z(t)) = \Re(A(t)e^{i\theta(t)}) = A(t)\cos\theta(t) \tag{6}$$

in which $\Re(\cdot)$ indicates the real part of a complex number. It is clear that, based on the HSA, $c(t)$ and its corresponding Hilbert transform, $y(t)$, is defined as $A(t)\cos\theta(t)$ and $A(\mathrm{t})\sin\theta(t)$, respectively. $A(t)$ is a positive-valued function and $\theta(t)$ is a monotone increasing function. If $c(t)$ represents an IMF, the original signal can be expressed as the following form:

$$x(t) = \Re\left\{\sum_{j=1}^{n} A_j(t)\, e^{i\int 2\pi f_j(t)dt}\right\} \tag{7}$$

In Eq. 7, $r_n(t)$ is deliberately omitted, because it is either a monotonic function, or a constant. Eq. 7 can be used to represent frequency-time distribution of the amplitude which is termed as the Hilbert spectrum, $H(f,t)$. Marginal Hilbert spectrum, $h(f)$, is also defined as follows:

$$h(f) = \int_0^T H(f,t)\, dt \tag{8}$$

Limitations of Hilbert spectral analysis

EMD procedure fulfills just necessary conditions for applying the HSA, but two unsatisfied requirements according to Bedrosian and Nuttall theorems still exist (Huang and Bethesda 2005). The Bedrosian theorem states that the Hilbert transform of a production of two functions; $A(t)$ and $\cos\theta(t)$, can be written as:

$$H\left[A(t)\cos\theta(t)\right] = A(t)H\left[\cos\theta(t)\right] \tag{9}$$

only if the Fourier spectra of $A(t)$ and $\cos\theta(t)$ are totally disjointed in frequency space, and if the frequency content of the spectrum of $\cos\theta(t)$ is higher than that of $A(t)$. If these requirements are satisfied, Eq. 6 is a correct definition. Otherwise, the phase and amplitude functions would mix together and the determined results are altered to falsify the values of instantaneous amplitudes and frequencies. On the other hand, Nuttall theorem states that if $\theta(t)$ is not a narrow band function but arbitrary function, $H[\cos\theta(t)]$ will not be necessarily $\sin\theta(t)$.

To satisfy the requirements of Bedrosian theorem, Huang and Bethesda (2005) proposed the normalized amplitude Hilbert transform (NAHT) method which involves the following steps: (1) extract IMFs from the signal, (2) connect all the local maxima for each IMF by a cubic spline interpolant as $A(t)$ (or instantaneous amplitude), (3) normalize each IMF by its instantaneous amplitude to obtain its carrier wave as the $\cos\theta(t)$, and (4) apply the Hilbert transform to each carrier wave to determine instantaneous frequency. Even if this method performs perfectly, the requirements of Nuttall theorem are not still fulfilled. Huang (2005) have proposed arc-cosine function as an alternative for Hilbert transform to calculate the phase function to satisfy the requirement of Nuttall theorem, but due to imperfect normalization in NAHT method, carrier wave can take values out of [–1,1], therefore the arc-cosine function cannot be correctly applied.

The enhanced Hilbert-Huang transform

In this section, to overcome the mentioned problems an enhanced HHT (EHHT) method is presented (Bahar and Ramezani 2009, Ramezani 2009). In EHHT method, Hilbert transform is replaced by a new procedure based on arc-cosine function, but an IMF is still considered as $A(t)\cos\theta(t)$. The EHHT is summarized in five steps as follows:

1) Perform the EMD to extract IMFs from the signal. For each IMF calculate the instantaneous amplitude, $A(t)$, based on the NAHT method.

2) For each IMF, normalize positive values by cubic spline interpolant through the local maxima and normalize negative values by absolute value of cubic spline interpolant through the local minima to get the imperfect carrier wave (Fig. 1 a). Determine perfect carrier wave by correcting the positive and negative values of the imperfect carrier wave applying *upper and lower corrective curves* (Fig. 1 b). Upper (lower) corrective curve is defined as a piecewise cubic polynomials which runs through the local maxima (minima) of the imperfect carrier wave with zero slope as shown in Fig. 1(a). Proposed correction is so infinitesimal that cannot affect the imperfect carrier wave considerably.

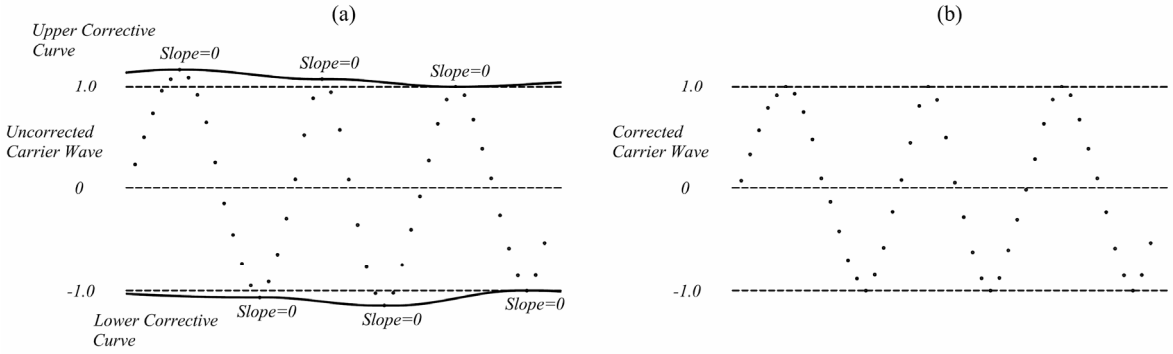

Figure 1. Correction of an imperfect carrier wave

3) Apply arc-cosine to the perfect carrier wave to determine the phase function, $\theta(t)$, as a monotone increasing function. This overcomes the limitation of the Nuttall theorem which restricts performance of the HSA. According to the definition, instantaneous frequency of an IMF can be achieved by calculating derivative of the phase function. But in most discrete cases, a noise contaminated phase function results in a physically meaningless frequency with a large dispersion.

4) Define a *cubic smoothing spline* function thtough the discrete noise contaminated phase functions as follows:

$$S(p) = p\sum_i w_i\left[y_i - C(x_i)\right]^2 + (1-p)\int \lambda(z)\,C''(z)^2 dz \tag{10}$$

where (x_i,y_i) is a set of knots, *i.e.* phase data, $C(x)$ is a cubic spline interpolant function, p is the smoothing parameter, w is a discrete uniform weighting vector and λ is a continuous uniform weighting function. In this study, the value of the uniform vector and function are assumed to be 1, and variation of p is examined. The basic interval of p is [0,1]. Very often, the range of interest for p is $p_h = 1/(1+h^3/6)$, where h is the average space between the x_is. But, it will be shown in the following section that p_h may not be a good choice for all physical situations. By applying $S(p)$ to the monotone increasing phase function shown in Fig. 2(a), a smoothed phase function is obtained shown in Fig. 2(b). Note that, smaller values of p results in a more smoothed phase function with less scattered frequency.

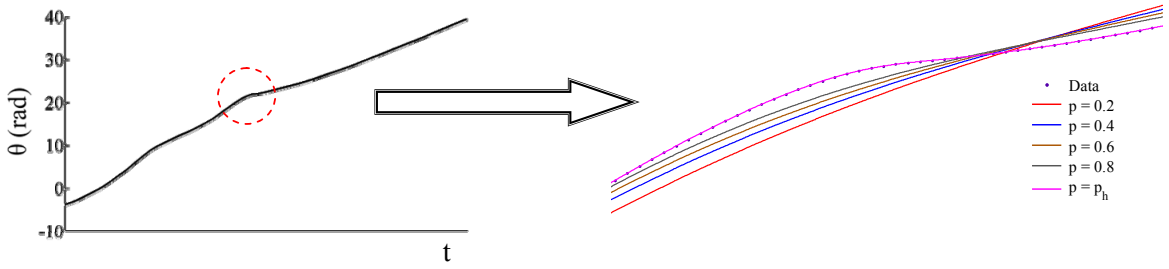

Figure 2. Effect of p on smoothing of a monotone increasing phase function

By taking derivative of the smoothed phase function, $\theta_s(t)$, instantaneous frequency of the IMF, f_s, is obtained:

$$f_S(t) = \frac{1}{2\pi}\frac{d\theta_S(t)}{dt} \tag{11}$$

5) Having instantaneous frequency and instantaneous amplitude for each IMF, enhanced spectrum of the signal, $E(f,p,t)$, can be determined. Also the marginal enhanced spectrum, $e(f,p)$, can be defined as follows:

$$e(f,p) = \int_0^T E(f,p,t)\,dt \tag{12}$$

In the next section, based on the EHHT an output-only system identification method is considered in detail.

A system identification method based on the enhanced Hilbert-Huang transform

In this section, based on EHHT an output-only system identification method is proposed to extract natural frequencies and their associated eigenvectors from the ambient response of structural systems. In the following, the procedure is explained for an arch bridge (Beichuan Bridge) in detail. Accuracy and reliability of the obtained results are verified using other valid methods which differ over their concepts and definitions.

The Beichuan bridge description

The Beichuan Bridge is a steel arch bridge with 90 m span located at the center of Xining City in China (Fig. 3). A field dynamic test was carried out using the ambient vibration technique just prior to the official opening of the bridge to traffic. The deck of the bridge is suspended through 32 main suspenders and measurement points were chosen on both sides of the bridge at a location near the joint of the suspenders and deck. Therefore, a total of 32 locations (16 points per side) were selected and measurements made there in vertical and transverse directions (Fig. 4). Four test set-ups in both directions were realized to cover the planned test area of the bridge. One reference location in each direction was selected near one side of the abutment for each set-up. Each set-up consisted of nine accelerometers (Fig. 4). Ambient excitations were used as sources of excitation during testing. The sampling rate on site for vertical data was 80 Hz. (Zong et al. 2005).

Figure 3. The Beichuan Bridge

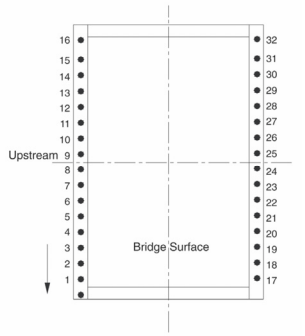

Figure 4. Arrangement of the measurement points

Identification of the natural frequencies

It is assumed that frequencies corresponding to the few first modes of the bridge are below 8 Hz; therefore the raw data are resampled to 16 Hz and EMD is applied thereafter. In the present case, all of the IMFs are not needed to be considered. Frequency-time distribution of the amplitude can lead us to choose sufficient number of IMFs. The spectra of the acceleration recorded in point 5 corresponding to the first five IMFs obtained by using HHT and EHHT are shown in Fig. 5. In addition to the limitations of HSA, wider frequency band in the few first IMFs (Flandrin et al. 2004) can decrease readability of the spectrum as it is occurred in Hilbert spectrum in Fig. 5(a) and in Fig. 5(b) with smoothing parameter equal to p_h in which amplitude distribution is not clear. By decreasing p, readability of the enhanced spectrum is increased as shown in Figs. 5(c), (d) and (e). This capability of the EHHT can help us to realize and extract the major characteristics of the complicated signals.

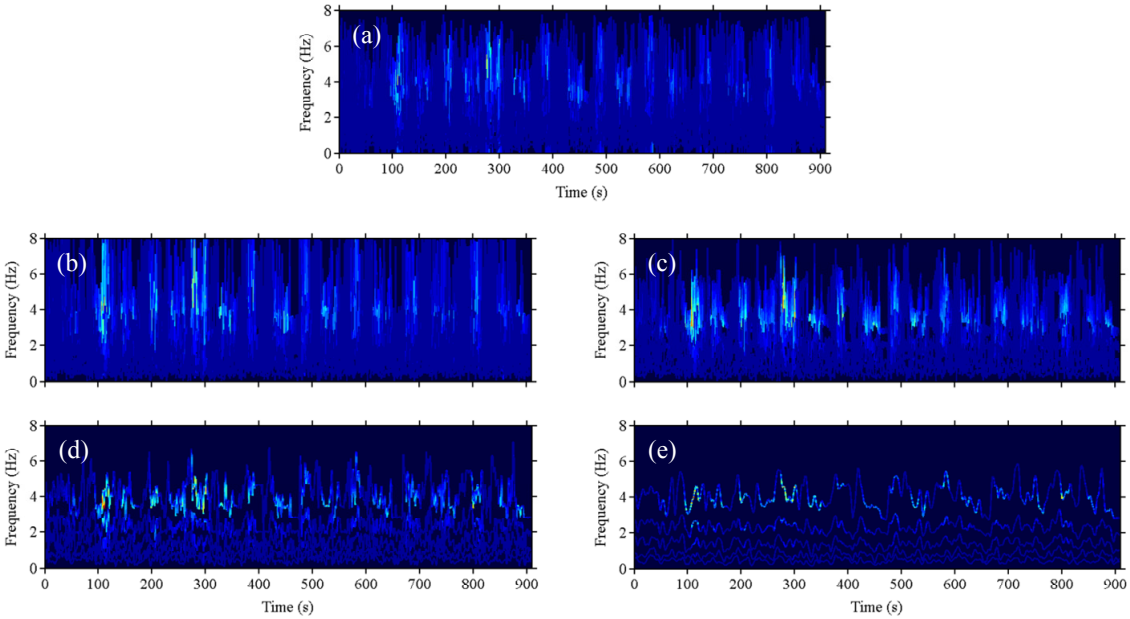

Figure 5. The spectra of measured response in point 5 using: (a) HHT, (b) EHHT, $p = p_h$, (c) EHHT, $p = 0.99$ (d) EHHT, $p = 0.50$ and (e) EHHT, $p = 0.01$

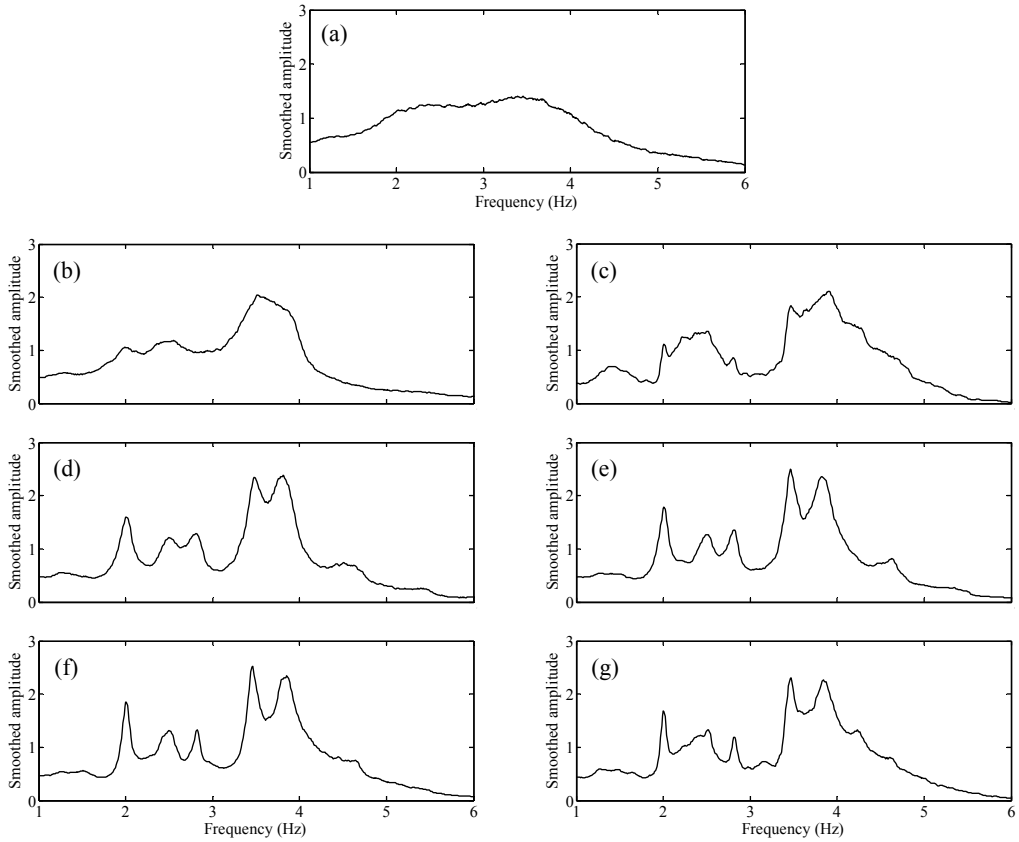

Figure 6. The smoothed averaged marginal spectrum using: (a) HHT, (b) EHHT, $p = p_h$, (c) $p = 0.99$ (d) $p = 0.70$ (e) $p = 0.50$ (f) $p = 0.30$ and (g) $p = 0.01$

Now, it can be seen that the first two IMFs carry majority of the energy (brighter colors) and the first five IMFs are sufficient to cover frequency range between 1 to 6 Hz. This trend can be observed for other recorded accelerations. To have a global picture of the natural frequencies, the marginal spectrum corresponding to each point is first calculated and then an *averaged marginal spectrum* is calculated by averaging between all of 32 marginal spectra. Averaged marginal spectra using HHT and EHHT are presented in Fig. 6. No sharp peaks are appeared in Fig. 6(a) due to both mentioned limitations and dispersion in frequency values that HHT suffers from. Similarly, marginal spectra in Figs 6(b) and (c) show no better results again due to dispersion in frequency caused by the smoothing parameter very close to 1.0, *i.e.* 0.99 and p_h. Figs 6(d), (e) and (f) show more stable spectra by the smoothing parameter equal to 0.7, 0.5, and 0.3, in which six sharp clear peaks can be easily identified. By decreasing the smoothing parameter close to 0, some unreal peaks are appeared caused by the smoothing parameter very near to 0 (Fig. 6 g). Extensive analysis shows that, there is not any predefined value for the smoothing parameter to achieve the best result and it is highly dependent on the case selection. Frequencies corresponding to peaks in Fig. 6(e) are designated as the natural frequencies of the bridge. Identified frequencies obtained by the proposed method and two other methods (PP and SSI methods) reported by Zong et al. (2005) are compared in Table 1. The identified results from these basically different methods show very good agreement among each other.

Table 1: Comparing the first six natural frequencies identified using the proposed method, PP method, and SSI method

Mode	Proposed method	PP	SSI
	Frequency (Hz)	Frequency (Hz)	Frequency (Hz)
1	2.01	2.012	2.002
2	2.51	2.519	2.511
3	2.82	2.812	2.827
4	3.46	3.457	3.473
5	3.83	3.926	3.864
6	4.64	4.628	–

Extraction of mode shapes

After approximation of the natural frequencies of the bridge mode shapes are extracted by a direct view on the modal response vectors. For an *n*-DOF system displacement and acceleration responses can be decomposed into *n* modes based on the generalized coordinates as follows:

$$\mathbf{X}(t) = \sum_{j=1}^{n} \mathbf{\Phi}_j v_j(t); \quad \ddot{\mathbf{X}}(t) = \sum_{j=1}^{n} \mathbf{\Phi}_j \ddot{v}_j(t) \tag{13}$$

in which $\mathbf{\Phi}_j$ is the *j*th modal vector, $v_j(t)$ are the *j*th generalized modal coordinates. We can find a good approximation for $\mathbf{\Phi}_j \ddot{v}_j(t)$ in each measurement point through band-pass filtering and applying EMD to the recorded acceleration responses. Based on the theory, if these

approximations are determined along the measurement points for the *j*th mode shape, their differences are only related to their modal components. Applying this idea to the recorded acceleration responses, an approximation for $\mathbf{\Phi}_j \ddot{v}_j(t)$ as $\mathbf{I}_j(t)$ is obtained. By choosing an appropriate normalizing point, *q*, the ratio of the absolute value of the modal elements $\phi_{i,j}$ and $\phi_{q,j}$ can be identified as:

$$|\phi_{i,j}| / |\phi_{q,j}| = \text{mean}\,[A_{i,j}(t) / A_{q,j}(t)] \qquad i = 1,2,...,n \tag{14}$$

in which $A_{i,j}(t)$ and $A_{q,j}(t)$ are the instantaneous amplitudes of $I_{i,j}(t)$ and $I_{q,j}(t)$, respectively. The mean value is used to decrease the noise level of the measured response. Since, sign of the ratio of $\phi_{i,j}$ and $\phi_{q,j}$ can be defined same as the sign of $\varphi_{ij,q}$ (which is related to the phase angle between the two functions) as follows:

$$\varphi_{ij,q} = \text{mean}\,[I_{i,j}(t) / I_{q,j}(t)] \tag{15}$$

Using the above mentioned procedure shape vectors for each set-up is extracted separately, in which $q = 6, 11, 22, 27$ are used for the set-ups one to four respectively. Identified mode shapes are shown in Fig. 7 that confirms those identified by Zong et al. (2005).

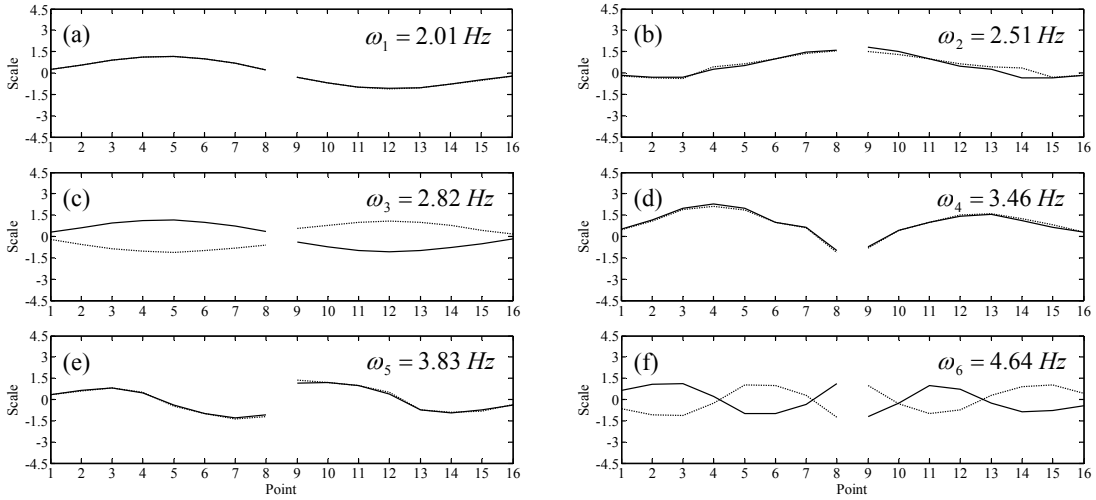

Figure 7. The first six mode shapes; (a) the 1st bending mode, (b) the 2nd bending mode, (c) the 1st torsional mode, (d) the 3rd bending mode, (e) the 4th bending mode, and (f) the 2nd torsional mode

Conclusions

First, a five-step procedure named enhanced Hilbert-Huang transform (EHHT) has been proposed in which limitations of the classical method in Hilbert spectral analysis is circumvented. Spectrum obtained from the EHHT offers improvement in frequency resolution and tracking ability. Second, based on the EHHT an output-only system identification method has been

proposed through a case study of an arch bridge. Natural frequencies are estimated from an averaged marginal spectrum and then corresponding mode shapes are extracted with a remarkable accuracy. In the proposed method, natural frequencies are validated by determination of their corresponding mode shapes. Results from the proposed method are in agreement with those from the SSI method. But the proposed method employs much simpler theoretical basis than the SSI method. Therefore, the proposed method is expected to be an effective tool for future research in system identification.

References

Bahar, O., Ramezani, S., 2009. Analysis of non stationary and nonlinear signals using a new enhanced Hilbert-Huang transform, *Signal Processing* (submitted).

Deering, R., and Kaiser, J. F., 2005. The use of a masking signal to improve empirical mode decomposition, *Proceedings of IEEE International Conference on Acoustics. Speech, and Signal Processing* 4, 485–488.

Flandrin, P., Rilling, G., and Goncalves, P., 2004. Empirical mode decomposition as a filter bank, *IEEE Signal Proc Let* 11, 112–114.

Huang, N. E., Shen, Z., Long, S.R., Wu, M. C., Shin, H. S., Zheng, Q., et al., 1998. The empirical mode decomposition and the Hilbert spectrum for nonlinear and non-stationary time series analysis, *Proc. R. Soc. London* 454, 903–995.

Huang, N. E., Shen, Z., and Long, S. R., 1999. A new view of nonlinear water waves: The Hilbert spectrum, *Annu. Rev. Fluid Mech* 31, 417–457.

Huang, N. E., 2005. Introduction to Hilbert-Huang transform and some recent developments, in: Huang N. E., and Attoh-Okine, N. O., Eds., *The Hilbert-Huang Transform in Engineering*, Taylor & Francis, Boca Raton.

Huang, N. E., and Bethesda, M. D., 2005. Computing instantaneous frequency by normalizing Hilbert transform, *US Patent* 6901353.

Ramezani, S., 2009. Developing a system identification process based on a new enhanced Hilbert-Huang transform, *MSc thesis*, International Institute of Earthquake Engineering and Seismology, Tehran.

Sharpley, R. C., and Vatchev, V., 2006. Analysis of the intrinsic mode functions, *Journal of Constructive Approximation* 24, 17–47.

Yang, J. N., Lei, Y., Pan, S., and Huang, N. E., 2003. System identification of linear structures based on Hilbert-Huang spectral analysis Part 1: normal modes, *Earthquake Engineering and Structural Dynamics* 32, 1443–1467.

Yang, J. N., Lei, Y., Lin, S., and Huang, N. E., 2004. Identification of Natural Frequencies and Dampings of In Situ Tall Buildings Using Ambient Wind Vibration Data, *Journal of Engineering Mechanics* 130, 570–577.

Zong, Z. H., Jaishi, B., Ge, J. P., and Ren, W. X., 2005. Dynamic analysis of a half-through concrete-filled steel tubular arch bridge. *Engineering Structures* 27, 3–15.